Observer-Based Feedback Controllers for Exponential Stabilization of Hybrid Periodic Orbits: Application to Underactuated Bipedal Walking*

Kaveh Akbari Hamed[1], Aaron D. Ames[2], and Robert D. Gregg[3]

***Abstract*— This paper presents a systematic approach to design observer-based output feedback controllers for hybrid dynamical systems arising from bipedal walking. We consider a class of parameterized observer-based output feedback controllers for exponential stabilization of hybrid periodic orbits. The properties of the Poincaré map are investigated to show that the Jacobian linearization of the Poincaré map takes a triangular form. This demonstrates the nonlinear separation principle for periodic orbits. In particular, the exponential stabilization of hybrid periodic orbits under dynamic output feedback control can be achieved by solving separate eigenvalue placement problems for the nonlinear state feedback and the observer. The paper then solves the state feedback and observer design problems by employing an iterative algorithm based on a sequence of optimization problems involving bilinear and linear matrix inequalities. The theoretical results are confirmed by designing a nonlinear observer-based output feedback controller for underactuated walking of a 3D humanoid model with 18 state variables, 54 state feedback parameters, and 271 observer parameters.**

I. INTRODUCTION

This paper provides the analytical foundation to systematically design observer-based output feedback controllers for hybrid dynamical systems arising from bipedal locomotion. The stabilization problem is addressed through the Poincaré sections analysis. Properties of the Poincaré return map are investigated to extend the nonlinear separation principle to hybrid periodic orbits. We employ an algorithm based on an iterative sequence of optimization problems involving linear and bilinear matrix inequalities (LMIs and BMIs) to synthesize the state feedback and observer. The proposed framework can overcome specific difficulties arising from the lack of a closed-form expression for the Poincaré map, high dimensionality, and underactuation in tuning observer-based nonlinear output controllers for legged robots.

Models of bipedal locomotion are hybrid with continuous-time dynamics representing the stance phases and discrete-time dynamics representing the impact events, that is, the nonstance legs contacting the walking surface. State-of-the-art nonlinear control approaches for bipedal walking such as the zero moment point [1], [2], controlled symmetries [3], hybrid reduction [4]–[6], transverse linearization [7], and hybrid zero dynamics (HZD) [8]–[10] assume that all state variables are available for feedback in real time. Among the above-mentioned approaches, the transverse linearization approach and HZD-based controllers deal with underactuation. HZD controllers have been validated numerically and experimentally for 2D and 3D bipedal robots [11]–[16], monopedal robots [17], quadruped robots [18], powered prosthetic legs [19]–[22], and exoskeletons [23]. In this approach, a set of output functions, referred to as virtual constraints, is defined for the continuous-time dynamics of the system and asymptotically driven to zero by the input-output (I-O) linearizing feedback controller [24]. Although legged robots are becoming more sophisticated with high degrees of freedom (DOF), the measurement of the entire state variables for feedback linearization becomes too expensive. Furthermore, it is not clinically feasible for human users of prosthetic legs to wear sensors at their intact joints. Hence, nonlinear control approaches for powered prosthetic legs, e.g., [19], primarily rely on high-gain controllers or expensive force sensors to deal with nonlinear interactions between the amputee body and robotic leg for feedback linearization. This underlines the need to systematically develop observer-based output feedback controllers to stabilize walking gaits for hybrid models of legged machines.

Existing observer design approaches for nonlinear dynamical systems, including hybrid systems, pertain to the estimation of state variables around *equilibrium points* and *not* periodic orbits. The design of an observer for nonlinear systems is a significant challenge. This challenge has been addressed in the literature of dynamical systems through the development of different techniques including Luenberger-like observers [25]–[27], the use of LMIs [25], [26], [28] and BMIs [29]–[31], and the use of high-gain observers [32]–[35]. There are several results that present the separation principle for *equilibrium points* of nonlinear systems [24], [26], [27], [32], [36]–[42]. Asymptotic observers that deal with *periodic gaits* of underactuated bipedal robots have been designed based on two different approaches. The first approach makes use of sliding mode observers to estimate the absolute orientation of planar (2D) bipedal robots when the robot's shape (i.e., internal joint) variables are measurable [43]–[45]. The second approach applies high gain full- and reduced-order observers to estimate generalized velocity components of bipedal robots when position variables are

*This material is based upon work supported by the National Science Foundation under Grant Number 1637704. The content is solely the responsibility of the authors and does not necessarily represent the official views of the NSF. R. D. Gregg holds a Career Award at the Scientific Interface from the Burroughs Wellcome Fund.

[1]K. Akbari Hamed is with the Department of Mechanical Engineering, San Diego State University, San Diego, CA 92182-1323 USA kakbarihamed@mail.sdsu.edu

[2]A. D. Ames is with the Department of Mechanical and Civil Engineering, California Institute of Technology, Pasadena, CA 91125 USA ames@cds.caltech.edu

[3]R. D. Gregg is with the Departments of Bioengineering and Mechanical Engineering, University of Texas at Dallas, Richardson, TX 75080-3021 USA rgregg@utdallas.edu

Preprint submitted to 2018 American Control Conference.
Received September 18, 2017.

measurable [46]. However, these approaches cannot address the general problem of designing observer-based output feedback controllers when a given set of measurements is available.

The contributions of this paper are as follows: 1) A class of parameterized, smooth, and nonlinear observer-based output feedback controllers is proposed; 2) The properties of the Poincaré map for the closed-loop models of dynamic walking are investigated; 3) It is shown the Jacobian linearization of the Poincaré map has a triangular structure that demonstrates the nonlinear separation principle for hybrid periodic orbits; 4) The state feedback and observer design problems are separately solved through application of an offline algorithm based on an iterative sequence of BMI optimization problems; and 5) The power of the analytical framework is ultimately illustrated through designing a set of HZD-based controllers integrated with an observer for dynamic walking of a 3D bipedal model with human parameters, 18 state variables, 3 degrees of underactuation, 54 state feedback control parameters, and 271 observer parameters.

II. HYBRID MODELS OF BIPEDAL WALKING

We consider single-phase hybrid dynamical systems arising from bipedal walking as follows

$$\Sigma^{\text{ol}}: \begin{cases} \dot{x} = f(x) + g(x)\,u, & x^- \notin \mathcal{S} \\ y = h(x) & \\ x^+ = \Delta(x^-), & x^- \in \mathcal{S}, \end{cases} \tag{1}$$

in which the superscript "ol" stands for the open-loop system, and $x \in \mathcal{X}$ and $u \in \mathcal{U}$ represent the *state variables* and *control inputs*, respectively. The *state manifold* and *set of admissible control inputs* are denoted by $\mathcal{X} \subset \mathbb{R}^n$ and $\mathcal{U} \subset \mathbb{R}^m$ for some positive integers n and m. The continuous-time portion of the hybrid system is given by the ordinary differential equation (ODE) $\dot{x} = f(x) + g(x)\,u$, where the vector field $f : \mathcal{X} \to \mathrm{T}\mathcal{X}$ and columns of g (i.e., g_j for $j = 1, \cdots, m$) are smooth (i.e., $\mathcal{C}^\infty$). In our notation, $\mathrm{T}\mathcal{X}$ denotes the *tangent bundle* of the state manifold $\mathcal{X}$. The *measurement vector* is given by $y = h(x) \in \mathbb{R}^\nu$ for some positive integer ν, in which $h : \mathcal{X} \to \mathbb{R}^\nu$ is a $\mathcal{C}^\infty$ mapping. The discrete-time portion of the hybrid system is represented by the *reset law* $x^+ = \Delta(x^-)$, where $\Delta : \mathcal{X} \to \mathcal{X}$ is a $\mathcal{C}^\infty$ *reset map*, and $x^-(t) := \lim_{\tau \nearrow t} x(\tau)$ and $x^+(t) := \lim_{\tau \searrow t} x(\tau)$ denote the left and right limits of the state trajectory $x(t)$, respectively. The guard of the hybrid system is then represented by the *switching manifold* $\mathcal{S} := \{x \in \mathcal{X} \,|\, s(x) = 0,\, \sigma(x) < 0\}$ on which the state solutions undergo an abrupt change according to the reset law. Here, $s : \mathcal{X} \to \mathbb{R}$ denotes a $\mathcal{C}^\infty$ *switching function* with the property $\frac{\partial s}{\partial x}(x) \neq 0$ for all $x \in \mathcal{S}$. Finally, $\sigma : \mathcal{X} \to \mathbb{R}$ is a $\mathcal{C}^\infty$ function to determine feasible switching events as $\sigma(x) < 0$.

Throughout this paper, we shall assume that there exists a period-one orbit for the hybrid system (1) that is transversal to $\mathcal{S}$. This notion can be expressed precisely as follows.

Assumption 1 (Transversal Period-One Orbit): There are a positive scalar $T^\star$ (referred to as the *fundamental period*), smooth *nominal state solution* $\varphi^\star : [0, T^\star] \to \mathcal{X}$, and smooth *nominal control input* $u^\star : [0, T^\star] \to \mathcal{U}$ such that 1) $\dot{\varphi}^\star(t) = f(\varphi^\star(t)) + g(\varphi^\star(t))\,u^\star(t)$ for all $t \in [0, T^\star]$; 2) $\varphi^\star(t) \notin \mathcal{S}$ for every $t \in [0, T^\star)$ and $\varphi^\star(T^\star) \in \mathcal{S}$; 3) $\varphi^\star(0) = \Delta(\varphi^\star(T^\star))$ (periodicity); and 4) $\dot{s}(\varphi^\star(T^\star)) = \frac{\partial s}{\partial x}(\varphi^\star(T^\star))\,\dot{\varphi}^\star(T^\star) \neq 0$ (transversality). Then, $\mathcal{O} := \{x = \varphi^\star(t) \,|\, 0 \leq t < T^\star\}$ is a *period-one* orbit transversal to the switching manifold $\mathcal{S}$. Furthermore, $\{x^\star\} := \overline{\mathcal{O}} \cap \mathcal{S}$ is a singleton, where $\overline{\mathcal{O}}$ denotes the set closure of the orbit $\mathcal{O}$.

Our objective is to systematically design nonlinear and time-invariant observer-based output controllers that exponentially stabilize the orbit $\mathcal{O}$ for the closed-loop system. For this purpose, we make use of the concept of the phasing variable. The *phasing variable* represents the system's (i.e., robot's) progression through the orbit (i.e., walking cycle), replacing the role of time in *time-invariant* feedback controllers. This becomes more precise in the following assumption.

Assumption 2 (Phasing Variable): There exists a $\mathcal{C}^\infty$ and real-valued function $\theta : \mathcal{X} \to \mathbb{R}$, referred to as the *phasing variable*, such that 1) $\mathrm{L}_g \mathrm{L}_f^i \theta(x) = 0$ for all $x \in \mathcal{X}$, $i = 0, 1, \cdots, r-1$ and some positive integer $r > 1$, and 2) $\theta(x)$ is strictly increasing function of time along the orbit $\mathcal{O}$, i.e., $\dot{\theta}(x) = \mathrm{L}_f \theta(x) > 0$ for all $x \in \overline{\mathcal{O}}$.

Reference [47] shows that Assumption 2 follows directly from Assumption 1 on the periodic orbit. For later purposes, the desired evolution of the state variables on the orbit $\mathcal{O}$ can be expressed in terms of the phasing variable θ as follows

$$x_{\text{d}}(\theta) := \varphi^\star(t)\,\big|_{t = \Theta^{-1}(\theta)}\,, \tag{2}$$

where $\theta = \Theta(t)$ and $t = \Theta^{-1}(\theta)$ represent the time profile of the phasing variable on the orbit $\mathcal{O}$ and its inverse function, respectively.

III. FAMILY OF PARAMETERIZED OBSERVER-BASED OUTPUT CONTROLLERS

This section presents a family of parameterized observer-based output feedback controllers to exponentially stabilize the periodic orbit $\mathcal{O}$. We consider a *general* class of nonlinear dynamic feedback controllers as follows

$$\Sigma^{\text{c}}: \begin{cases} \dot{\hat{x}} = f(\hat{x}) + g(\hat{x})\,u + L(\eta)\,(y(x) - y(\hat{x})) \\ u = \Gamma(\hat{x}, \xi), & x^- \notin \mathcal{S} \\ \hat{x}^+ = \Delta(\hat{x}^-), & x^- \in \mathcal{S} \end{cases} \tag{3}$$

which is parameterized by 1) a set of *adjustable* controller parameters $\xi \in \Xi \subset \mathbb{R}^{p_c}$ and 2) a set of *adjustable* observer parameters $\eta \in \mathbb{R}^{p_o}$ for some positive integers p_c and p_o. Here, the superscript "c" stands for the controller and $\Xi \subset \mathbb{R}^{p_c}$ represents the *set of admissible controller parameters*. In (3), we consider a full-order observer dynamics whose structure is taken from [46]. The observer consists of a copy of the continuous- and discrete-time dynamics of the original model (1) plus measurement injection. The switching condition for the observer dynamics is expressed in terms of the impact instants of the original system. In particular, we assume that the switching events of the system (1) are detectable. This assumption is *not* restrictive for models of

Preprint submitted to 2018 American Control Conference.
Received September 18, 2017.

bipedal machines as one can detect the impact events using the contact sensors attached to the leg ends. In (3), $\hat{x}$ and $\hat{y} := y(\hat{x})$ represent the *estimates* of the state vector x and measurement vector y, respectively. The observer gain matrix is then denoted by $L(\eta) \in \mathbb{R}^{n\times\nu}$ which is parameterized by η. Finally, $\Gamma : \mathcal{X} \times \Xi \to \mathcal{U}$ is a $\mathcal{C}^\infty$ state feedback law parameterized by the controller parameters ξ. Throughout this paper, we shall assume that the following *invariance condition* is satisfied.

Assumption 3 (Invariant Periodic Orbit): The family of state feedback laws $u = \Gamma(x, \xi)$ preserves the orbit $\mathcal{O}$ for the following parameterized closed-loop hybrid system

$$\Sigma^{\text{cl}}_{\xi} : \begin{cases} \dot{x} = f(x) + g(x)\,\Gamma(x,\xi), & x^- \notin \mathcal{S} \\ x^+ = \Delta(x^-), & x^- \in \mathcal{S}, \end{cases} \tag{4}$$

in which the superscript "cl" stands for the closed-loop system. In particular, $\frac{\partial}{\partial \xi}\Gamma(x,\xi) = 0$ for all $(x,\xi) \in \overline{\mathcal{O}} \times \Xi$, i.e., $\Gamma(\varphi^\star(t),\xi) = u^\star(t)$ for every $t \in [0, T^\star]$ and $\xi \in \Xi$.

Assumption 3 states that $\mathcal{O}$ is an *invariant* periodic orbit for the closed-loop hybrid system (4) under the change of the controller parameters $\xi \in \Xi$. This condition helps us to preserve the orbit $\mathcal{O}$ while looking for a stabilizing set of controller parameters in Section V.

Example 1: (Partial Feedback Linearizing Laws): We consider an important family of state feedback laws satisfying the invariance condition. Let us consider the following *parameterized controlled functions* to be regulated for the continuous-time dynamics of (1):

$$z(x,\xi) := H(\xi)\,(x - x_{\text{d}}(\theta)), \tag{5}$$

where $\dim(z) = \dim(u) = m$, and $H(\xi) \in \mathbb{R}^{m\times n}$ denotes the *controlled matrix* to be determined and parameterized by ξ. One possible parameterization is to assume that $\xi := \text{vec}(H) \in \mathbb{R}^{p_c}$, where "vec" denotes the vectorization operator and $p_c := mn$. We further suppose that the controlled function z has uniform relative degree r with respect to u on an open neighborhood of $\mathcal{O}$ for $\xi \in \Xi \subset \mathbb{R}^{p_c}$. The partial feedback linearizing law then takes the form

$$\Gamma(x,\xi) = -\left(\text{L}_g \text{L}_f^{r-1} z\right)^{-1} \left(\text{L}_f^r z + \sum_{j=0}^{r-1} k_j\, \text{L}_f^j z\right), \tag{6}$$

where the constants k_j for $j = 0, 1, \cdots, r-1$ are chosen such that the monic polynomial $\lambda^r + k_{r-1}\lambda^{r-1} + \cdots + k_1\lambda + k_0$ becomes Hurwitz. Applying the partial feedback linearizing controller results in the controlled function dynamics $z^{(r)} + \sum_{j=0}^{r-1} k_j\, z^{(j)} = 0$ for which the origin is exponentially stable. Reference [48, Example 2] shows that the feedback law (6), restricted to $\mathcal{O}$, is invariant under the choice of ξ. That is, $\frac{\partial \Gamma}{\partial \xi}(x,\xi) = 0$ for all $(x,\xi) \in \overline{\mathcal{O}} \times \Xi$, and hence, the invariance condition is satisfied.

IV. EXPONENTIAL STABILIZATION UNDER DYNAMIC OUTPUT FEEDBACK CONTROL

The objective of this section is to investigate the properties of the Poincaré map to extend the separation principle for exponential stabilization of hybrid periodic orbits.

A. Augmented Closed-Loop Dynamics

By defining the *estimation error* $e := x - \hat{x} \in \mathbb{R}^n$, we can express the augmented closed-loop hybrid system in the (x, e) coordinates as follows

$$\Sigma^{\text{cl}}_{\xi,\eta} : \begin{cases} \begin{bmatrix} \dot{x} \\ \dot{e} \end{bmatrix} = \begin{bmatrix} f^{\text{cl}}(x,e,\xi) \\ v(x,e,\xi,\eta) \end{bmatrix}, & x^- \notin \mathcal{S} \\ \begin{bmatrix} x^+ \\ e^+ \end{bmatrix} = \begin{bmatrix} \Delta(x^-) \\ w(x^-, e^-) \end{bmatrix}, & x^- \in \mathcal{S}, \end{cases} \tag{7}$$

in which

$$f^{\text{cl}}(x,e,\xi) := f(x) + g(x)\,\Gamma(x-e,\xi) \tag{8}$$

$$\begin{aligned} v(x,e,\xi,\eta) := {} & f(x) - f(x-e) \\ & + g(x)\,\Gamma(x-e,\xi) - g(x-e)\,\Gamma(x-e,\xi) \\ & - L(\eta)\,(y(x) - y(x-e)) \end{aligned} \tag{9}$$

$$w(x,e) := \Delta(x) - \Delta(x-e). \tag{10}$$

To simplify the notation, one can present the augmented system (7) in a compact form as follows

$$\Sigma^{\text{cl}}_{\xi,\eta} : \begin{cases} \dot{x}_a = f_a^{\text{cl}}(x_a,\xi,\eta), & x_a^- \notin \mathcal{S}_a \\ x_a^+ = \Delta_a(x_a^-), & x_a^- \in \mathcal{S}_a, \end{cases} \tag{11}$$

where $x_a := (x^\top, e^\top)^\top \in \mathcal{X}_a$, $\mathcal{X}_a := \mathcal{X} \times \mathbb{R}^n$, and $\mathcal{S}_a := \mathcal{S} \times \mathbb{R}^n$ represent the *augmented state variables*, *augmented state manifold*, and *augmented switching manifold*, respectively. The augmented closed-loop vector field and reset map are also defined as $f_a^{\text{cl}}(x_a,\xi,\eta) := \left(f^{\text{cl}\top}(x,e,\xi), v^\top(x,e,\xi,\eta)\right)^\top$ and $\Delta_a(x_a) := \left(\Delta^\top(x), w^\top(x,e)\right)^\top$, in which the subscript "a" stands for the augmented system. For later purposes, the unique solution of the smooth and augmented closed-loop ODE $\dot{x}_a = f_a^{\text{cl}}(x_a,\xi,\eta)$ with the initial condition $x_a(0) := (x^\top(0), e^\top(0))^\top \in \mathcal{X}_a$ is denoted by

$$\varphi_a(t, x_a(0), \xi, \eta) := \begin{bmatrix} \varphi_x(t, x_a(0), \xi, \eta) \\ \varphi_e(t, x_a(0), \xi, \eta) \end{bmatrix}$$

for all $t \geq 0$ in the maximal interval of existence, where the subscripts "x" and "e" represent the x- and e-components of the solution, respectively. The *time-to-switching function*, $T : \mathcal{X}_a \times \Xi \times \mathbb{R}^{p_o} \to \mathbb{R}_{>0}$, is then defined as the first time at which the flow $\varphi_a(t, x_a(0), \xi, \eta)$ intersects the augmented switching manifold $\mathcal{S}_a$, i.e.,

$$T(x_a(0),\xi,\eta) := \inf\{t > 0 \,|\, \varphi_a(t, x_a(0), \xi, \eta) \in \mathcal{S}_a\}.$$

The following lemma presents some fundamental properties of the augmented closed-loop hybrid system.

Lemma 1: (Properties of the Closed-Loop System): Assume that Assumptions 1-3 are satisfied. Then, the following statements are correct.

1) $v(x, 0, \xi, \eta) = 0$ for all $(x,\xi,\eta) \in \mathcal{X} \times \Xi \times \mathbb{R}^{p_o}$.
2) For all $(\xi,\eta) \in \Xi \times \mathbb{R}^{p_o}$,

$$\begin{aligned} \mathcal{O}_a &:= \mathcal{O} \times \{0\} \\ &= \left\{ x_a = \varphi_a^\star(t) := \begin{bmatrix} \varphi^\star(t) \\ 0 \end{bmatrix} \,\middle|\, 0 \leq t < T^\star \right\} \end{aligned}$$

Preprint submitted to 2018 American Control Conference.
Received September 18, 2017.

is an invariant period-one orbit for $\Sigma^{\rm cl}_{\xi,\eta}$ which is transversal to $\mathcal{S}_a$.

Proof: Part (1) is immediate. From Part (1) and the fact that $w(x,0)=0$ for all $x\in\mathcal{X}$, one can conclude that $\mathcal{O}_a$ is a period-one orbit. By defining the augmented switching function $s_a(x_a):=s(x)$ and $x_a^\star:=(x^{\star\top},0)^\top$, we observe that $\frac{\partial s_a}{\partial x_a}(x_a^\star)f_a^{\rm cl}(x_a^\star,\xi,\eta)=\frac{\partial s}{\partial x}(x^\star)\,f^{\rm cl}(x^\star,0,\xi)\neq 0$ for all (ξ,η) which completes the proof. ∎

B. Augmented Poincaré Map

To study the stabilization problem, we make use of *Poincaré section analysis*. By taking the Poincaré section as the augmented switching manifold $\mathcal{S}_a$, the evolution of $\Sigma^{\rm cl}_{\xi,\eta}$ on $\mathcal{S}_a$ can be described by the following discrete-time system

$$x_a[k+1]=P_a\left(x_a[k],\xi,\eta\right),\quad k=0,1,\cdots, \tag{12}$$

where $P_a:\mathcal{S}_a\times\Xi\times\mathbb{R}^{p_o}\to\mathcal{S}_a$ defined by

$$\begin{aligned}P_a(x_a,\xi,\eta)&:=\begin{bmatrix}P\left(x,e,\xi,\eta\right)\\ Q\left(x,e,\xi,\eta\right)\end{bmatrix}\\ &:=\varphi_a\left(T\left(\Delta_a\left(x_a\right),\xi,\eta\right),\Delta_a\left(x_a\right),\xi,\eta\right)\end{aligned}$$

represents the *parameterized and augmented Poincaré map*. According to the invariance condition, $x_a^\star$ is an *invariant fixed point* for P_a under the change of the controller and observer parameters, that is, $P_a\left(x_a^\star,\xi,\eta\right)=x_a^\star$ for all $(\xi,\eta)\in\Xi\times\mathbb{R}^{p_o}$. Linearization of the discrete-time system (12) around $x_a^\star$ then results in

$$\delta x_a[k+1]=\frac{\partial P_a}{\partial x_a}\left(x_a^\star,\xi,\eta\right)\delta x_a[k] \tag{13}$$

where $\delta x_a[k]:=x_a[k]-x_a^\star$.

Problem 1 (Exponential Stability): The problem of exponential stabilization of the periodic orbit $\mathcal{O}_a$ consists of finding the controller and observer parameters (ξ,η) such that the Jacobian matrix $\frac{\partial P_a}{\partial x_a}\left(x_a^\star,\xi,\eta\right)$ becomes Hurwitz.

For later purposes, we define the compact notation for the Jacobian matrix as $A(\xi,\eta):=\frac{\partial P_a}{\partial x_a}(x_a^\star,\xi,\eta)$.

C. Nonlinear Separation Principle for Periodic Orbits

Theorem 1: (Separation Principle for Hybrid Periodic Orbits): Assume that Assumptions 1-3 are satisfied. Then, the Jacobian matrix $A(\xi,\eta)$ has an upper triangular structure as follows:

$$A(\xi,\eta)=\begin{bmatrix}A_{11}(\xi) & A_{12}(\xi,\eta)\\ 0 & A_{22}(\eta)\end{bmatrix}, \tag{14}$$

where $A_{11}:=\frac{\partial P}{\partial x}(x^\star,0,\xi,\eta)$, $A_{12}:=\frac{\partial P}{\partial e}(x^\star,0,\xi,\eta)$, and $A_{22}:=\frac{\partial Q}{\partial e}(x^\star,0,\xi,\eta)$. Furthermore, the submatrices $A_{11}(\xi)$ and $A_{22}(\eta)$ are only functions of the controller and observer parameters, respectively.

Remark 1: Theorem 1 presents an upper triangular structure for the Jacobian linearization of the augmented Poincaré map. This demonstrates the nonlinear separation principle for hybrid periodic orbits, i.e., exponential stabilization of periodic orbits under the dynamic output feedback control (3) can be achieved by solving separate eigenvalue placement problems for the nonlinear state feedback and the observer. That is, $\text{eig}(A(\xi,\eta))=\text{eig}(A_{11}(\xi))\cup\text{eig}(A_{22}(\eta))$.

Proof: Let us define the Jacobian matrix of the augmented vector field along the orbit $\mathcal{O}_a$ as follows:

$$\begin{aligned}J_a\left(t,\xi,\eta\right)&:=\frac{\partial f_a^{\rm cl}}{\partial x_a}\left(x_a,\xi,\eta\right)\Big|_{x_a=\varphi_a^\star(t)}\\ &=\begin{bmatrix}\frac{\partial f^{\rm cl}}{\partial x}\left(x,e,\xi\right) & \frac{\partial f^{\rm cl}}{\partial e}\left(x,e,\xi\right)\\ \frac{\partial v}{\partial x}\left(x,e,\xi,\eta\right) & \frac{\partial v}{\partial e}\left(x,e,\xi,\eta\right)\end{bmatrix}\Bigg|_{x=\varphi^\star(t),e=0}\end{aligned}$$

for all $(t,\xi,\eta)\in[0,T^\star]\times\Xi\times\mathbb{R}^{p_o}$. Now we consider the following linear time-varying matrix differential equation, referred to as the variational equation (VE),

$$\begin{aligned}&\dot\Phi_a\left(t,\xi,\eta\right)=J_a\left(t,\xi,\eta\right)\Phi_a\left(t,\xi,\eta\right),\quad 0\le t\le T^\star\\ &\Phi_a\left(0,\xi,\eta\right)=I,\end{aligned} \tag{15}$$

where $\Phi_a(t,\xi,\eta)=\frac{\partial\varphi_a}{\partial x_a(0)}(t,x_a(0),\xi,\eta)\in\mathbb{R}^{2n\times 2n}$ represents the *trajectory sensitivity matrix* for the closed-loop ODE $\dot x_a=f_a^{\rm cl}(x_a,\xi,\eta)$. According to [49, Appendix B], the Jacobian matrix of the augmented Poincaré map, i.e., $A(\xi,\eta)$, can be expressed as

$$A\left(\xi,\eta\right)=\Pi_a\,\Phi_a\left(T^\star,\xi,\eta\right)D_a, \tag{16}$$

in which Π_a represents the saltation matrix for the augmented closed-loop system defined by

$$\Pi_a:=I-\frac{f_a^{\rm cl}\left(x_a^\star,\xi,\eta\right)\frac{\partial s_a}{\partial x_a}\left(x_a^\star\right)}{\frac{\partial s_a}{\partial x_a}\left(x_a^\star\right)f_a^{\rm cl}\left(x_a^\star,\xi,\eta\right)}. \tag{17}$$

Furthermore, D_a denotes the Jacobian matrix of the augmented reset map, evaluated at $x_a^\star$, i.e., $D_a:=\frac{\partial\Delta_a}{\partial x_a}\left(x_a^\star\right)$. In what follows, we will study the properties of the three matrices in (16).

According to the construction procedure, one can show that the saltation matrix Π_a and the reset map Jacobian D_a take block diagonal forms as follows:

$$\begin{aligned}\Pi_a&=\text{block diag}\left\{\Pi_{11},I\right\}\\ D_a&=\text{block diag}\left\{D_{11},D_{11}\right\},\end{aligned} \tag{18}$$

where $\Pi_{11}:=I-\frac{f^{\rm cl}(x^\star,0,\xi)\frac{\partial s}{\partial x}(x^\star)}{\frac{\partial s}{\partial x}(x^\star)f^{\rm cl}(x^\star,0,\xi)}$ and $D_{11}:=\frac{\partial\Delta}{\partial x}\left(x^\star\right)$. Moreover from the invariance condition in Assumption 3, Π_{11} and D_{11} are *independent* of the choice of the controller and observer parameters (ξ,η). Next, we focus on the VE given in (15). From Part (1) of Lemma 1, $\frac{\partial v}{\partial x}(x,0,\xi,\eta)\equiv 0$, and hence, one can conclude that the Jacobian matrix $J_a(t,\xi,\eta)$ has an upper triangular structure as follows:

$$J_a(t,\xi,\eta)=\begin{bmatrix}J_{11}(t,\xi) & J_{12}(t,\xi)\\ 0 & J_{22}(t,\eta)\end{bmatrix}, \tag{19}$$

in which

$$\begin{aligned}J_{11}\left(t,\xi\right)&:=\frac{\partial f^{\rm cl}}{\partial x}\left(x,e,\xi\right)\Big|_{x=\varphi^\star(t),e=0}\\ &=\frac{\partial}{\partial x}\left(f(x)+g(x)\,\Gamma\left(x,\xi\right)\right)\Big|_{x=\varphi^\star(t)}\\ J_{12}\left(t,\xi\right)&:=\frac{\partial f^{\rm cl}}{\partial e}\left(x,e,\xi\right)\Big|_{x=\varphi^\star(t),e=0}\\ &=-g(x)\frac{\partial\Gamma}{\partial x}\left(x,\xi\right)\Big|_{x=\varphi^\star(t)}\end{aligned}$$

are solely functions of the controller parameters ξ. Furthermore, we claim that J_{22} only depends on the observer parameters η. To observe this, we remark that

$$\begin{aligned} J_{22}(t,\eta) &:= \frac{\partial v}{\partial e}(x,e,\xi,\eta)\Big|_{x=\varphi^\star(t),e=0} \\ &= \frac{\partial f}{\partial x}(x)\Big|_{x=\varphi^\star(t)} \\ &+ \sum_{j=1}^{m} g_j(x)\left(\frac{\partial \Gamma_j}{\partial x}(x,\xi) - \frac{\partial \Gamma_j}{\partial x}(x,\xi)\right)\Big|_{x=\varphi^\star(t)} \\ &+ \sum_{j=1}^{m} \frac{\partial g_j}{\partial x}(x)\,\Gamma_j(x,\xi)\Big|_{x=\varphi^\star(t)} \\ &- L(\eta)\,\frac{\partial y}{\partial x}(x)\Big|_{x=\varphi^\star(t)} \\ &= \frac{\partial f}{\partial x}(x)\Big|_{x=\varphi^\star(t)} + \sum_{j=1}^{m} \frac{\partial g_j}{\partial x}(x)\Big|_{x=\varphi^\star(t)} u_j^\star(t) \\ &- L(\eta)\,\frac{\partial y}{\partial x}(x)\Big|_{x=\varphi^\star(t)}, \end{aligned} \tag{20}$$

in which we have made use of the invariance condition in the sixth line of (20) as $\Gamma_j(\varphi^\star(t),\xi) = u_j^\star(t)$ for all $\xi \in \Xi$ and $u^\star(t)$ is the nominal control input defined in Assumption 1.

Now we study the structure of the trajectory sensitivity matrix. According to the triangular structure of the Jacobian matrix $J_a(t,\xi,\eta)$ in (19) and the VE in (15), we can decompose the trajectory sensitivity matrix as follows:

$$\Phi_a(t,\xi,\eta) := \begin{bmatrix} \Phi_{11}(t,\xi) & \Phi_{12}(t,\xi,\eta) \\ 0 & \Phi_{22}(t,\eta) \end{bmatrix}, \tag{21}$$

where $\Phi_{11}(t,\xi) := \frac{\partial \varphi_x}{\partial x(0)}(t,x_a(0),\xi,\eta)$, $\Phi_{12}(t,\xi,\eta) := \frac{\partial \varphi_x}{\partial e(0)}(t,x_a(0),\xi,\eta)$, and $\Phi_{22}(t,\eta) := \frac{\partial \varphi_e}{\partial e(0)}(t,x_a(0),\xi,\eta)$ satisfying the following matrix differential equations

$$\begin{aligned} \dot\Phi_{11}(t,\xi) &= J_{11}(t,\xi)\,\Phi_{11}(t,\xi), \quad \Phi_{11}(0,\xi) = I \\ \dot\Phi_{22}(t,\eta) &= J_{22}(t,\eta)\,\Phi_{22}(t,\eta), \quad \Phi_{22}(0,\eta) = I \\ \dot\Phi_{12}(t,\xi,\eta) &= J_{11}(t,\xi)\,\Phi_{12}(t,\xi,\eta) \\ &\quad + J_{12}(t,\xi)\,\Phi_{22}(t,\eta), \quad \Phi_{12}(0,\xi,\eta) = 0. \end{aligned}$$

Finally, substituting (18) and (21) into (16) completes the proof of (14) for which

$$A_{11}(\xi) = \Pi_{11}\,\Phi_{11}(T^\star,\xi)\,D_{11} \tag{22}$$

$$A_{12}(\xi,\eta) = \Pi_{11}\,\Phi_{12}(T^\star,\xi,\eta)\,D_{11} \tag{23}$$

$$A_{22}(\eta) = \Phi_{22}(T^\star,\eta)\,D_{11}. \tag{24}$$

■

V. ITERATIVE BMI ALGORITHM FOR THE EXPONENTIAL STABILIZATION PROBLEM

The objective of this section is to solve the state feedback and observer design problems through application of an iterative algorithm based on a sequence of optimization problems involving BMIs. Our previous work has developed the BMI algorithm to systematically choose stabilizing state feedback laws from a family of parameterized controllers [48], [50], [51]. In addition, we have numerically and experimentally validated the algorithm in designing nonlinear state feedback controllers for walking of 3D underactuated bipedal robots [52], [53]. In this paper, we show that the BMI algorithm can be employed to design observer-based output feedback controllers.

A. Stability as Nonlinear Matrix Inequalities

The separation principle in Section IV-C enables us to synthesize the observer-based output feedback control (3) by looking for the controller and observer parameters (i.e., ξ and η) such that the eigenvalues of $A_{11}(\xi)$ and $A_{22}(\eta)$ lie inside the unit circle. In particular from Theorem 1 and [51, Eqs. 2-4], we can express Problem 1 in terms of the following two nonlinear matrix inequalities (NMIs):

$$\text{Controller Design:} \quad \mathcal{I}(A_{11}(\xi),W_1,\gamma_1) > 0,\ \gamma_1 > 0 \tag{25}$$

$$\text{Observer Design:} \quad \mathcal{I}(A_{22}(\eta),W_2,\gamma_2) > 0,\ \gamma_2 > 0, \tag{26}$$

where

$$\mathcal{I}(A_{ii},W_i,\gamma_i) := \begin{bmatrix} W_i & A_{ii}\,W_i \\ \star & (1-\gamma_i)\,W_i \end{bmatrix} > 0, \quad i \in \{1,2\} \tag{27}$$

represents a matrix inequality to guarantee that the eigenvalues of A_{ii} lie inside the unit circle. Specifically, $V(x) = x^\top W_i^{-1} x$ is a Lyapunov candidate function for $x[k+1] = A_{ii}\,x[k]$ such that $V[k+1] - V[k] < -\gamma_i\,V[k]$, in which $0 < \gamma_i < 1$ is a scalar to tune the convergence rate.

B. Iterative BMI Algorithm

The BMI algorithm provides a sequence of observer parameters $\{\eta^0,\eta^1,\cdots\}$ for the observer synthesis (resp., controller parameters $\{\xi^0,\xi^1,\cdots\}$ for the state feedback synthesis) that eventually solves (26) (resp. (25)). In our notation, the superscript $\ell \in \{0,1,\cdots\}$ denotes the iteration number. During iteration ℓ of the algorithm, the Jacobian matrix $A_{22}\left(\eta^\ell + \Delta\eta\right)$ (resp. $A_{11}\left(\xi^\ell + \Delta\xi\right)$) is replaced by its first-order approximation, based on the Taylor series expansion, which is affine in $\Delta\eta$ (resp., $\Delta\xi$). Here, $\Delta\eta$ (resp. $\Delta\xi$) is a sufficiently small increment in the observer (resp. controller) parameters and the approximate Jacobian matrix is shown by $\hat A_{22}\left(\eta^\ell,\Delta\eta\right)$ (resp. $\hat A_{11}\left(\xi^\ell,\Delta\xi\right)$). Next, we replace $A_{22}\left(\eta^\ell + \Delta\eta\right)$ (resp., $A_{11}\left(\xi^\ell + \Delta\xi\right)$) in the NMI (27) by the first-order approximation. This will yield a BMI condition in terms of $(\Delta\eta,W_2,\gamma_2)$ (resp., $(\Delta\xi,W_1,\gamma_1)$) rather than an NMI condition which can be solved with available software packages such as PENBMI [54]. In particular, we solve the following BMI problem for the observer synthesis:

$$\min_{(\Delta\eta,W_2,\gamma_2,\delta)} \quad -w\,\gamma_2 + \delta \tag{28}$$

$$\text{s.t.} \quad \mathcal{I}\left(\hat A_{22}\left(\eta^\ell,\Delta\eta\right),W_2,\gamma_2\right) > 0,\ \gamma_2 > 0 \tag{29}$$

$$\begin{bmatrix} I & \Delta\eta \\ \star & \delta \end{bmatrix} > 0, \tag{30}$$

Preprint submitted to 2018 American Control Conference.
Received September 18, 2017.

where from the Schur complement lemma and LMI (30), δ is an uper bound on the 2-norm of $\Delta\eta$, i.e., $\delta > \|\Delta\eta\|_2^2$. Furthermore, $w > 0$ is a weighting factor as a trade-off between improving the convergence rate (i.e., minimizing $(1-\gamma_2)$) and minimizing $\|\Delta\eta\|_2^2$ to have a good first-order approximation. An analogous BMI optimization problem can be presented for the state feedback synthesis. The local minimum solution (*not* necessarily the global solution) of the BMI optimization problem is then used to update the observer (resp., controller) parameters as $\eta^{\ell+1} = \eta^{\ell} + \Delta\eta$ (resp., $\xi^{\ell+1} = \xi^{\ell} + \Delta\xi$)) for the next iteration. We have presented sufficient conditions for the convergence of the algorithm to a stabilizing set of parameters at a finite number of iterations in [50, Theorem 2]. In addition, an effective numerical approach to compute the first-order approximation of the Jacobian matrix has been developed in [48, Theorem 2]. Finally we remark that if the BMI optimization is not feasible, the algorithm is not successful and stops.

VI. APPLICATION TO 3D UNDERACTUATED BIPEDAL WALKING

This section confirms the analytical results by designing observer-based output feedback controllers for dynamic walking of a 3D underactuated bipedal robot.

A. 3D Underactuated Bipedal Robot

The model of the robot consists of a rigid tree structure with a torso and two identical legs terminating at point feet (see Fig. 1). Each leg of the robot includes 3 actuated DOFs: a 2 DOF (ball) hip joint with roll and pitch angles plus a 1 DOF knee joint in the sagittal plane. During the single support phase, the robot has 9 DOFs with 6 actuators. We remark that the roll, pitch, and yaw angles associated with the torso frame are unactuated. The kinematic and dynamic parameter values for the links are taken according to those reported in [55] from a human cadaver study. A minimal set of configuration variables for the robot, shown by q, consists of the yaw, roll, and pitch angles for the torso plus a set of six relative angles to describe the shape of the mechanical system. The state vector is also represented by $x := \left(q^\top, \dot{q}^\top\right)^\top \in \mathcal{X} \subset \mathbb{R}^{18}$. Using the motion planning algorithm of [15], a periodic gait $\mathcal{O}$ is designed for walking at 0.6 (m/s) with the cost of mechanical transport CMT $= 0.07$.

B. State Feedback Controller Design

Virtual constrains are kinematic relations among the generalized coordinates enforced asymptotically by continuous-time feedback control [11]–[16], [19]–[23], [48]. They are defined to coordinate the links of the bipedal robot within a stride. In this paper, we consider a set of parameterized virtual constraints as follows:

$$z\left(x,\xi\right) := H\left(\xi\right)\left(q - q_{\mathrm{d}}\left(\theta\right)\right), \tag{31}$$

in which $q_{\mathrm{d}}(\theta)$ represents the desired evolution of the configuration variables on the desired gait $\mathcal{O}$ in terms of the phasing variable. The virtual constraints are then enforced by the I-O linearizing feedback laws of (6) for which the uniform relative degree r is assumed to be 2. The stability of the walking gait in the virtual constraints approach depends on the choice of the output matrix $H(\xi) \in \mathbb{R}^{6\times 9}$ [48]. To stabilize the gait, we employ the iterative BMI algorithm to look for stabilizing controller parameters $\xi = \mathrm{vec}(H) \in \Xi \subset \mathbb{R}^{54}$. To solve the BMI optimization problem at each iteration of the algorithm, we make use of the PENBMI solver from TOMLAB [56] integrated with the MATLAB environment through YALMIP [57]. BMIs are nonconvex and NP-hard problems [58]. However, PENBMI is a general-purpose solver for BMIs, which guarantees the convergence to a local optimal point satisfying the Karush-Kuhn-Tucker optimality conditions. The BMI algorithm starts with an initial set of controller parameters ξ^0 for which $H\left(\xi^0\right) q$ represents the actuated position variables. For this set of controller parameters, the dominant eigenvalues and spectral radius of the 17×17 Jacobian matrix A_{11} become $\{-4.0307, -1.000, 0.7915, -0.262\}$ and 4.0307, respectively, and hence, the gait is unstable. After four iterations, the algorithm successfully converges to a stabilizing set of virtual constraints for which the dominant eigenvalues and spectral radius of A_{11} become $\{0.1624 \pm 0.7446i, 0.5309, -0.4176\}$ and 0.7621, respectively.

C. Observer Design

Motivated by future applications in prosthetic control where the joints of the human body do not have encoders, we assume that there is an array of five IMUs attached to the links of the kinematic chain (torso, right and left femurs, and right and left tibias). We further suppose that the available measurements for the system (i.e., y) only include the roll, pitch, and yaw signals from these five sensors, i.e., $y = h(x) \in \mathbb{R}^{15}$ (no relative angle and no velocity measurement). The relation between the minimal set of configuration variables $q \in \mathbb{R}^9$ and the position measurements from the IMU network, denoted by $\bar{q} := h(x) \in \mathbb{R}^{15}$, can then be expressed by a nonlinear function as follows:

$$q = F\left(\bar{q}\right) \tag{32}$$

for which there is *not* a closed-form expression according to the inverse kinematics techniques. The objective of this section is to design a full-order observer to estimate $(q, \dot{q})$ while measuring $\bar{q}$ and using the state feedback $\Gamma(q, \dot{q}, \xi)$. We remark that the high-gain observer of [46] cannot be employed to solve this problem. Instead, we will see that the BMI optimized observer can asymptotically solve (32), and hence, one does not need to design an alternative state feedback in terms of $(\bar{q}, \dot{\bar{q}})$ for exponential stabilization of walking gaits.

In this paper, the observer gain is taken as

$$L := \frac{1}{\epsilon} L_0 \in \mathbb{R}^{18\times 15}, \tag{33}$$

where $0 < \epsilon < 1$ is a sufficiently small number. The observer parameters then consist of the columns of L_0 and ϵ, that is, $\eta := \left(\mathrm{vec}(L_0)^\top, \epsilon\right)^\top \in \mathbb{R}^{271}$. We note that ϵ helps the BMI algorithm search for high-gain observers

Preprint submitted to 2018 American Control Conference.
Received September 18, 2017.

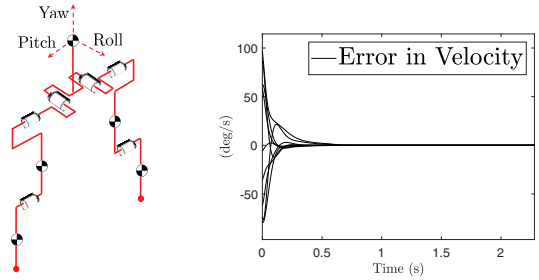

Fig. 1: The 3D robot model together with the estimation errors in the velocity components over the first 5 steps of 3D walking with the BMI optimized output feedback controller.

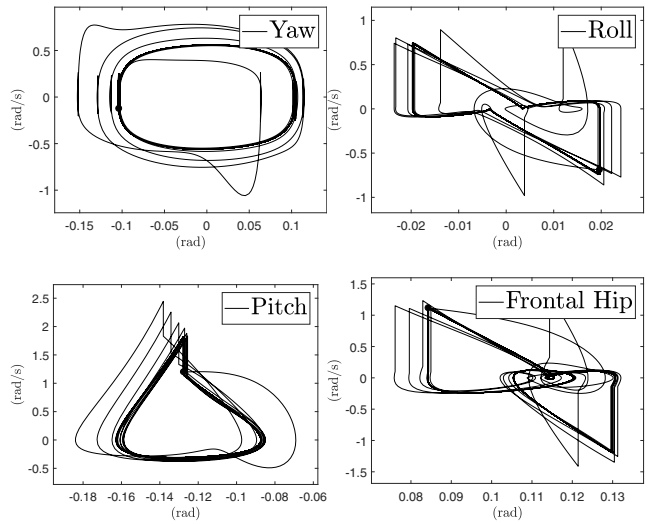

Fig. 2: Phase portraits for the torso Euler angles (yaw, roll, and pitch) and frontal hip during 100 consecutive steps of 3D walking with the BMI optimized output feedback controller.

in case needed. The BMI algorithm starts from an initial set of observer parameters for which the dominant eigenvalues and spectral radius of the 18×18 Jacobian matrix A_{22} are $\{26.8856, 0.1129, -0.0095, 0.0079\}$ and 26.8856, respectively[1]. The algorithm successfully converges to a set of stabilizing observer parameters after 19 iterations for which the spectral radius of A_{22} becomes 0.0053. Figures 1 and 2 illustrate the estimation error in the velocity components versus time and phase portraits for the BMI optimized closed-loop system, respectively. Here, the simulation starts off of the orbit at the beginning of the right stance phase with an estimation error of 90% in the velocity components. Convergence to the periodic orbit even in the yaw component is clear. The animation of this simulation together with the optimal controller and observer parameters can be found at [59].

VII. CONCLUSIONS

This paper introduced a systematic algorithm to design observer-based output feedback controllers that exponentially stabilize periodic orbits of hybrid dynamical systems. A class of parameterized output feedback controllers with full-order observers is assumed. The properties of the Poincaré map are investigated to show that the Jacobian linearization of the Poincaré map around the fixed point of the orbit has a triangular structure. This extends the nonlinear separation problem to hybrid periodic orbits. The paper then employs an iterative sequence of optimization problems involving BMIs to synthesize the state feedback and observer. The power of the analytical approach is finally confirmed by designing an observer-based output feedback controller for 3D underactuated walking of a humanoid model with 18 state variables, 54 controller parameters, and 271 observer parameters. For future work, we will investigate the design of $\mathcal{H}_2$- and $\mathcal{H}_\infty$-optimal observer-based output feedback controllers for robust stabilization of dynamic walking. We will also investigate the minimal sets of required sensors to achieve stable walking for models of autonomous robots and amputee locomotion.

[1]We remark that the augmented Poincaré map is 35-dimensional.

REFERENCES

[1] A. Goswami, "Postural Stability of Biped Robots and the Foot-Rotation Indicator (FRI) Point," *The International Journal of Robotics Research*, vol. 18, no. 6, pp. 523–533, 1999.

[2] M. Vukobratović, B. Borovac, and D. Surla, *Dynamics of Biped Locomotion*. Springer, 1990.

[3] M. Spong and F. Bullo, "Controlled symmetries and passive walking," *Automatic Control, IEEE Transactions on*, vol. 50, no. 7, pp. 1025–1031, July 2005.

[4] A. Ames and S. Sastry, "Hybrid geometric reduction of hybrid systems," in *Decision and Control, 45th IEEE Conference on*, Dec 2006, pp. 923–929.

[5] A. Ames, R. W. Sinnet, and E. D. Wendel, "Three-dimensional kneed bipedal walking: A hybrid geometric approach," in *Hybrid Systems: Computation and Control*, ser. Lecture Notes in Computer Science, R. Majumdar and P. Tabuada, Eds. Springer Berlin Heidelberg, 2009, vol. 5469, pp. 16–30.

[6] A. Ames, R. Gregg, and M. Spong, "A geometric approach to three-dimensional hipped bipedal robotic walking," in *Decision and Control, 46th IEEE Conference on*, Dec 2007, pp. 5123–5130.

[7] I. Manchester, U. Mettin, F. Iida, and R. Tedrake, "Stable dynamic walking over uneven terrain," *The International Journal of Robotics Research*, vol. 30, no. 3, pp. 265–279, 2011.

[8] E. Westervelt, J. Grizzle, and D. Koditschek, "Hybrid zero dynamics of planar biped walkers," *Automatic Control, IEEE Transactions on*, vol. 48, no. 1, pp. 42–56, Jan 2003.

[9] E. Westervelt, J. Grizzle, C. Chevallereau, J. Choi, and B. Morris, *Feedback Control of Dynamic Bipedal Robot Locomotion*. Taylor & Francis/CRC, 2007.

[10] B. Morris and J. Grizzle, "Hybrid invariant manifolds in systems with impulse effects with application to periodic locomotion in bipedal robots," *Automatic Control, IEEE Transactions on*, vol. 54, no. 8, pp. 1751–1764, Aug 2009.

[11] C. Chevallereau, G. Abba, Y. Aoustin, F. Plestan, E. Westervelt, C. Canudas-de Wit, and J. Grizzle, "RABBIT: a testbed for advanced control theory," *Control Systems Magazine, IEEE*, vol. 23, no. 5, pp. 57–79, Oct 2003.

[12] K. Sreenath, H.-W. Park, I. Poulakakis, and J. Grizzle, "Embedding active force control within the compliant hybrid zero dynamics to achieve stable, fast running on MABEL," *The International Journal of Robotics Research*.

[13] A. E. Martin, D. C. Post, and J. P. Schmiedeler, "The effects of foot geometric properties on the gait of planar bipeds walking under HZD-based control," *The International Journal of Robotics Research*, vol. 33, no. 12, pp. 1530–1543, 2014.

[14] J. Lack, M. Powell, and A. Ames, "Planar multi-contact bipedal walking using hybrid zero dynamics," in *Robotics and Automation, IEEE International Conference on*, May 2014, pp. 2582–2588.

[15] A. Ramezani, J. Hurst, K. Akbai Hamed, and J. Grizzle, "Performance analysis and feedback control of ATRIAS, a three-dimensional bipedal robot," *Journal of Dynamic Systems, Measurement, and Control December, ASME*, vol. 136, no. 2, December 2013.

Preprint submitted to 2018 American Control Conference.
Received September 18, 2017.

[16] A. Hereid, E. A. Cousineau, C. M. Hubicki, and A. D. Ames, "3D dynamic walking with underactuated humanoid robots: A direct collocation framework for optimizing hybrid zero dynamics," in *2016 IEEE International Conference on Robotics and Automation (ICRA)*, May 2016, pp. 1447–1454.

[17] I. Poulakakis and J. Grizzle, "The spring loaded inverted pendulum as the hybrid zero dynamics of an asymmetric hopper," *Automatic Control, IEEE Transactions on*, vol. 54, no. 8, pp. 1779–1793, Aug 2009.

[18] Q. Cao and I. Poulakakis, "Quadrupedal running with a flexible torso: control and speed transitions with sums-of-squares verification," *Artificial Life and Robotics*, vol. 21, no. 4, pp. 384–392, Dec 2016.

[19] R. Gregg, T. Lenzi, L. Hargrove, and J. Sensinger, "Virtual constraint control of a powered prosthetic leg: From simulation to experiments with transfemoral amputees," *Robotics, IEEE Transactions on*, vol. 30, no. 6, pp. 1455–1471, Dec 2014.

[20] R. Gregg and J. Sensinger, "Towards biomimetic virtual constraint control of a powered prosthetic leg," *Control Systems Technology, IEEE Transactions on*, vol. 22, no. 1, pp. 246–254, Jan 2014.

[21] A. Martin and R. Gregg, "Hybrid invariance and stability of a feedback linearizing controller for powered prostheses," in *American Control Conference*, 2015, pp. 4670–4676.

[22] H. Zhao, J. Horn, J. Reher, V. Paredes, and A. Ames, "Multicontact locomotion on transfemoral prostheses via hybrid system models and optimization-based control," *IEEE Transactions on Automation Science and Engineering*, vol. 13, no. 2, pp. 502–513, April 2016.

[23] A. Agrawal, O. Harib, A. Hereid, S. Finet, M. Masselin, L. Praly, A. Ames, K. Sreenath, and J. Grizzle, "First steps towards translating hzd control of bipedal robots to decentralized control of exoskeletons," *IEEE Access*, vol. 5, pp. 9919–9934, 2017.

[24] A. Isidori, *Nonlinear Control Systems*. Springer; 3rd edition, 1995.

[25] G. Ciccarella, M. D. Mora, and A. Germani, "A Luenberger-like observer for nonlinear systems," *International Journal of Control*, vol. 57, no. 3, pp. 537–556, 1993.

[26] R. Rajamani, "Observers for Lipschitz nonlinear systems," *IEEE Transactions on Automatic Control*, vol. 43, no. 3, pp. 397–401, Mar 1998.

[27] M. Arcak and P. Kokotovic, "Nonlinear observers: A circle criterion design and robustness analysis," *Automatica*, vol. 37, no. 12, pp. 1923 – 1930, 2001.

[28] A. Zemouche and M. Boutayeb, "On LMI conditions to design observers for Lipschitz nonlinear systems," *Automatica*, vol. 49, no. 2, pp. 585 – 591, 2013.

[29] Y. Wang and R. Rajamani, "Feasibility analysis of the bilinear matrix inequalities with an application to multi-objective nonlinear observer design," in *2016 IEEE 55th Conference on Decision and Control (CDC)*, Dec 2016, pp. 3252–3257.

[30] K. Goh, M. Safonov, and J. Ly, "Robust synthesis via bilinear matrix inequalities," *International Journal of Robust Nonlinear Control*, vol. 6, no. 9-10, pp. 1079–1095, 1996.

[31] J. VanAntwerp and R. Braatz, "A tutorial on linear and bilinear matrix inequalities," *Journal of Process Control*, vol. 10, no. 4, pp. 363–385, August 2000.

[32] A. Atassi and H. Khalil, "A separation principle for the stabilization of a class of nonlinear systems," *IEEE Transactions on Automatic Control*, vol. 44, no. 9, pp. 1672–1687, Sep 1999.

[33] J. Ahrens and H. Khalil, "High-gain observers in the presence of measurement noise: A switched-gain approach," *Automatica*, vol. 45, no. 4, pp. 936 – 943, 2009.

[34] A. A. Prasov and H. K. Khalil, "A nonlinear high-gain observer for systems with measurement noise in a feedback control framework," *IEEE Transactions on Automatic Control*, vol. 58, no. 3, pp. 569–580, March 2013.

[35] R. G. Sanfelice and L. Praly, "On the performance of high-gain observers with gain adaptation under measurement noise," *Automatica*, vol. 47, no. 10, pp. 2165 – 2176, 2011.

[36] A. Krener and A. Isidori, "Linearization by output injection and nonlinear observers," *Systems & Control Letters*, vol. 3, no. 1, pp. 47 – 52, 1983.

[37] S. Raghavan and J. Hedrick, "Observer design for a class of nonlinear systems," *International Journal of Control*, vol. 59, no. 2, pp. 515–528, 1994.

[38] J. P. Gauthier, H. Hammouri, and S. Othman, "A simple observer for nonlinear systems applications to bioreactors," *IEEE Transactions on Automatic Control*, vol. 37, no. 6, pp. 875–880, Jun 1992.

[39] A. Teel and L. Praly, "Global stabilizability and observability imply semi-global stabilizability by output feedback," *Syst. Control Lett.*, vol. 22, no. 5, pp. 313–325, May 1994.

[40] M. Maggiore and K. M. Passino, "A separation principle for a class of non-UCO systems," *IEEE Transactions on Automatic Control*, vol. 48, no. 7, pp. 1122–1133, July 2003.

[41] M. Arcak, "Certainty-equivalence output-feedback design with circle-criterion observers," *IEEE Transactions on Automatic Control*, vol. 50, no. 6, pp. 905–909, June 2005.

[42] B. Akmee and M. Corless, "Observers for systems with nonlinearities satisfying incremental quadratic constraints," *Automatica*, vol. 47, no. 7, pp. 1339 – 1348, 2011.

[43] V. Lebastard, Y. Aoustin, F. Plestan, and L. Fridman, "Absolute orientation estimation based on high order sliding mode observer for a five link walking biped robot," in *Variable Structure Systems, 2006. VSS'06. International Workshop on*, June 2006, pp. 373–378.

[44] V. Lebastard, Y. Aoustin, and F. Plestan, "Observer-based control of a walking biped robot without orientation measurement," *Robotica*, vol. 24, no. 3, pp. 385–400, May 2006.

[45] ——, "Step-by-step sliding mode observer for control of a walking biped robot by using only actuated variables measurement," in *2005 IEEE/RSJ International Conference on Intelligent Robots and Systems*, Aug 2005, pp. 559–564.

[46] J. W. Grizzle, J. H. Choi, H. Hammouri, and B. Morris, "On observer-based feedback stabilization of periodic orbits in bipedal locomotion," in *Methods and Models in Automation and Robotics*, August 2007, pp. 27–30.

[47] S. Burden, S. Revzen, and S. Sastry, "Model reduction near periodic orbits of hybrid dynamical systems," *Automatic Control, IEEE Transactions on*, vol. 60, no. 10, pp. 2626–2639, Oct 2015.

[48] K. Akbari Hamed, B. Buss, and J. Grizzle, "Exponentially stabilizing continuous-time controllers for periodic orbits of hybrid systems: Application to bipedal locomotion with ground height variations," *The International Journal of Robotics Research*, vol. 35, no. 8, pp. 977–999, 2016.

[49] T. Parker and L. Chua, *Practical Numerical Algorithms for Chaotic Systems*. Springer, 1989.

[50] K. Akbari Hamed and R. D. Gregg, "Decentralized feedback controllers for robust stabilization of periodic orbits of hybrid systems: Application to bipedal walking," *Control Systems Technology, IEEE Transactions on*, vol. 25, no. 4, pp. 1153–1167, July 2017.

[51] K. Akbari Hamed and J. W. Grizzle, "Reduced-order framework for exponential stabilization of periodic orbits on parameterized hybrid zero dynamics manifolds: Application to bipedal locomotion," *Nonlinear Analysis: Hybrid Systems*, vol. 25, pp. 227–245, August 2017.

[52] B. Buss, K. Akbari Hamed, B. A. Griffin, and J. W. Grizzle, "Experimental results for 3D bipedal robot walking based on systematic optimization of virtual constraints," in *2016 American Control Conference (ACC)*, July 2016, pp. 4785–4792.

[53] Dynamic Leg Locomotion YouTube Channel. (2015) MARLO: Dynamic 3D walking based on HZD gait design and BMI constraint selection, https://www.youtube.com/watch?v=5ms5DtPNwHo.

[54] D. Henrion, J. Lofberg, M. Kocvara, and M. Stingl, "Solving polynomial static output feedback problems with PENBMI," in *Decision and Control, and European Control Conference. 44th IEEE Conference on*, Dec 2005, pp. 7581–7586.

[55] P. de Leva, "Adjustments to Zatsiorsky-Seluyanov's segment inertia parameters," *J Biomech*, vol. 29, no. 9, pp. 123–1230, 1996.

[56] TOMLAB optimization, http://tomopt.com/tomlab/.

[57] J. Lofberg, "YALMIP: a toolbox for modeling and optimization in MATLAB," in *Computer Aided Control Systems Design, 2004 IEEE International Symposium on*, Sept 2004, pp. 284–289.

[58] O. Toker and H. Ozbay, "On the NP-hardness of solving bilinear matrix inequalities and simultaneous stabilization with static output feedback," in *American Control Conference, Proceedings of the 1995*, vol. 4, Jun 1995, pp. 2525–2526 vol.4.

[59] (2017) Observer-Based Feedback Controllers for Exponential Stabilization of Dynamic Walking, https://youtu.be/htdXWnFrWMw.